Macromolecules

Article

pubs.acs.org/Macromolecules

Static and Dynamic Large Strain Properties of Methyl Cellulose Hydrogels

Yonatan Rotbaum,*[,†] Galit Parvari,[‡] Yoav Eichen,[‡] and Daniel Rittel[†]

[†]Faculty of Mechanical Engineering and [‡]Schulich Faculty of Chemistry, Technion, 3200008 Haifa, Israel

Supporting Information

ABSTRACT: Methyl cellulose (MC) hydrogels display thermoreversible gelation upon heating. These hydrogels are abundantly employed in a variety of applications, rendering study of their mechanical properties relevant and important. Here we report on their basic elastic properties, based on ultrasonic measurements, and focusing on the heated solid gel, their mechanical properties in the quasi-static and dynamic (impact) large strain regimes are characterized. Unlike most other solids which soften upon heating, we find that methyl cellulose gels toughen increasingly on heating beyond the gelation point. Flow stress curves reveal polymer concentration dependent hardening. Contrary to most other soft materials, MC hydrogels do not present strain-rate sensitivity in the quasi-static range. Nevertheless, a dramatic change is observed in the dynamic regime, where at strain rates of ~1500 s^{-1} a 10−20-fold increase in flow strength is observed relative to the quasi-static regime. The results of this investigation complement the existing body of knowledge on the rheological properties of MC gels, extending the characterization to their large-strain, strain-rate dependent properties. Techniques presented in this work could be applied to examine other soft materials, and the characteristics found for methyl cellulose hydrogels could assist in advancing its employment in numerous applications.

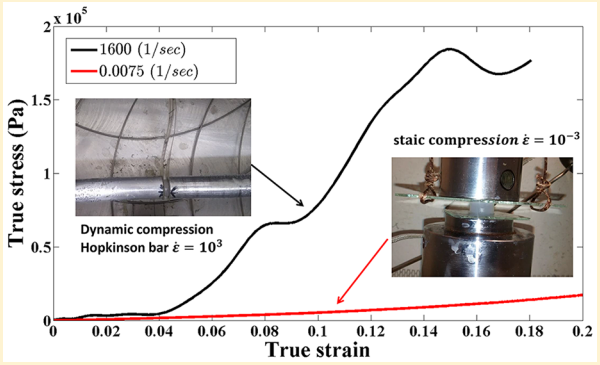

INTRODUCTION

The past decade is witnessing extensive interest in hydrogels,[1,2] which are increasingly finding their way into several fields such as industrial, agricultural, and consumer products as well as in biotechnology and pharma. Their various applications range from bulkhead seals[3] and microsensors,[4] through diapers, hair gels, and perfumes, to pollutant absorption, protein purification, and tissue engineering.[5−7] In many of these, the mechanical characteristics of the hydrogel are directly relevant to the practicability of the application.

Methyl cellulose (MC) based hydrogels, synthesized from the abundant and biorenewable cellulose, can be found in a wide range of applications, benefiting from their nontoxicity and biocompatibility.[8] These hydrogels display thermoreversible gelation, whereby upon heating the viscous liquid transforms into a solid-like gel phase. This fascinating phenomenon has been observed for only few materials and mixtures,[9] among which perhaps the most famous is poly(*N*-isopropylacrylamide) (PNIPAm)[10] whose phases separate above a lower critical solution temperature by an entropically driven process.[11] In the case of MC, the gelation occurs at atmospheric pressure and at a temperature T_g that is normally around 20−80 °C, which makes it relevant to many everyday applications.[12] Throughout the past decades, important studies on this phenomenon have been carried out to elucidate its mechanism,[13−16] kinetics,[17] and the rheological properties of the liquid and gel states.[18−20] The T_g itself has been found to depend on a number of factors among which are the degree of methylation, polymer concentration, applied shear, and presence of salts and other additives.[8,19,21−26] The aqueous solutions of MC undergo several temperature and structure dependent processes, such as changing solvation modes, weak supramolecular clustering of polymer chains, and formation of fibrillar structures which change their traits at temperatures considerably lower than T_g.[15,16,27,28]

Since this system undergoes spontaneous solidification upon heating, with a negative Gibbs free energy for this change (exergonic reaction), and since previous studies have shown this transition to be endothermic,[14] the entropy change, of this solidification must be positive.[29,30] Therefore, MC gels are characterized by higher entropy than their liquid counterparts, which is an abnormality in the realm of solids.[31] This characteristic has aroused our curiosity regarding the mechanical properties of the solids of such materials.

Changes in the gel with increase in temperature are not commonly studied. A report on **A4C** type MC-based hydrogels shows that more than one gel type is accessible (clear and turbid) at certain concentrations by temperature change.[13] The structure of MC hydrogels has remained elusive for a long time. Recent studies reveal an intriguing structure based on likely

Received: February 5, 2017
Revised: June 5, 2017

DOI: 10.1021/acs.macromol.7b00270
Macromolecules XXXX, XXX, XXX−XXX

nematic−isotropic[28] phase separation and a morphology of nanometer diameter fibrils forming network structures.[32,33] The mechanism of formation of these fibrils has in the past year become clearer with the development of simulations based on the coarse-grained model,[34] showing that depending on their substitution and length, MC polymers collapse to ring structures under heating.[35] In turn, these ring structures form tubes and then fibrils corresponding to the experimental observations, according to molecular dynamics and statistical mechanical modeling.[36] These fibrillar structures are attributed to the reported transitions, from shear thinning to shear thickening behavior, at the gelation point.[20] Furthermore, reports on the semiflexible nature of coiled MC polymers[37,38] prompt interest in exploring the influence of these molecular traits on the macroscale mechanical behavior.

MC-based gels possess a relatively low flow stress on the order of kPa, and therefore the experimental determination of their mechanical properties at large strains poses a significant experimental challenge.[39−45] Several reports are available on the mechanical properties of firmer gels, such as alginate,[46] composite bacterial hydrogels,[47] hydrogels with poly(vinyl alcohol) components,[48,49] and anisotropic hydrogels.[50] Some mechanical properties of cellulose derivatives have been reported in the literature[51−53] as well as hydrogels with MC components.[54,55] However, although there have been reports on powders[56] and films[57,58] of methyl cellulose, to our knowledge, the compressive mechanical response of the heated MC-based hydrogel itself at large strains has not been thoroughly studied. A single report describes the strength of two MC gels showing that the more concentrated one is stronger, but the focus of that study was placed on gels in which other components were added.[59] The approach encountered so far in the literature concerning the mechanical properties of MC based solution and gels is based on rheology. While this approach is highly valuable for studying processes in the solution and mechanisms leading to gelation, it is rather limited when one wishes to analyze the large strain mechanical properties of the gelled state, namely their stress−strain relationship over a wide range of strain rates.

This report consists of three main parts. In the first, we use ultrasonic measurements to characterize the basic elastic properties of the hydrogels' liquid and gel states: compressibility coefficient, Young's modulus, and Poisson's ratio.

Second, the quasi-static compression characteristics of two types of methyl cellulose hydrogels, Methocel (**A7C**) and medium viscosity Methocel (**A15C**), are explored. The mechanical response of the gels is characterized with respect to MC concentration, temperature, and strain rate.

The third part reports on the dynamic (high strain rate) compression response of **A7C** gels (solid state), using a modified Kolsky apparatus[60] also known as split Hopkinson pressure bar.[61]

EXPERIMENTAL DETAILS

Materials. Methyl cellulose type A15C Methocel (**A15C**, Sigma-Aldrich) and methyl cellulose SG **A7C** Food grade (**A7C**, generously provided by DOW Chemical Company) were used as received without further purification. Manufacturer reported values for percentage of methylation and viscosity of a 2% solution in water at 20 °C are 27.5−31.5% (DS 1.64−1.92) and 1200−1800 cP for **A15C** and 29.5−31.5% (DS 1.78−1.92) and 525−980 cP for **A7C**. Water was purified by a Millipore Milli-Q instrument reaching resistance of 18 MΩ.

Since the T_g can vary significantly with the heating rate,[22] gelation temperatures for the MC-based hydrogels in the heating rates used in this work, 10 °C/min, were measured by cloud point[62] (90% optical transference reduction, red-light LED in pulse mode (200 mA) set at 10 cm from a det10A SI-biased photodiode detector (Thorlabs) with an added amplification of ×50, with a thermocouple inserted into the hydrogel into a sealed vial). These temperatures are detailed in Table 1.

Table 1. T_g at a Heating Rate of 10 °C/min for the MC-Based Hydrogels in This Study (Variance up to ±2 °C)

concentration/MC type (g/L)	**A7C** (T_g, °C)	**A15C** (T_g, °C)
56	42	57
44	46	61
28	49	64

Gel Preparation. Weighed MC powder was added to the treated water at 70 °C in a capped vial equipped with a magnetic stirring bar. The suspension was mixed vigorously using a spatula, and then the vial was recapped and placed in a water bath at 70 °C for at least 10 min while stirring. The stirring bar was then removed, and the capped vial was placed in an ice bath for 60 min, during which the white opaque solution turns transparent and homogeneous. The solution is then stored for at least 12 h in 1−4 °C before measurements.

The concentration of the gels presented herein is nominal, according to the weight of the polymer introduced into the water, prior to gelation. For example, 56 g/L represents 0.28 g of MC added to 5 mL of water. However, due to the rapid heating the samples undergo before compression (see Static Compression subsection), a volume of low-concentration solution of up to 0.02 mL may be exuded from the gel (5 mL sample). This syneresis therefore leads to a maximal possible growth in concentration by 4%, which is not included in the nominal concentration value (so that the 56 g/L sample may have a maximum concentration of 58 g/L).

Ultrasonic Group Velocity. The ultrasonic experimental setup used for group velocity measurements consists of a high-voltage ultrasonic pulser (Olympus 5058PR) and two ultrasonic piezo-electric probes and two ultrasonic piezo-electric probes: one for exciting and receiving longitudinal waves at a nominal frequency of 1 MHz (SIUI-1M-24) and one for exciting and receiving shear stress waves at nominal frequency of 5 MHz (Olympus V152-RB). The measured ultrasonic signals were recorded using an oscilloscope (Agilent DSO-X 2004A, 2 GSa/s).

The ultrasonic measurements of the gels were performed using the pulse-echo technique.[63−65] The liquid gel was cast into a cylindrical PMMA holder, D = 40 mm with a thin (0.2 mm) plastic slide as under plate, which was practically transparent to the ultrasonic pulse and returning signals.

The raw data from each measurement includes at least four repetitive pulse echoes which were converted into rectified mode using Hilbert transform.[66] A homemade Matlab code[67] detects the location of the maximum amplitude of each pulse echo and calculates the group velocity (longitudinal/shear) using eq 1

$$V_g = \frac{2X}{t} \tag{1}$$

where X is the sample height and t is the time between two consecutive peaks.

For the MC gel state, the Young's modulus (E) and Poisson's ratio (ν) can be calculated from the measured shear and longitudinal wave velocities according to eq 2[63,68]

$$E = \frac{V_L^2 \rho(1+\nu)(1-2\nu)}{1-\nu}$$
$$\nu = \frac{1-2(V_T - V_L)^2}{2-2(V_T - V_L)^2} \tag{2}$$

where V_L and V_T are the longitudinal and the shear wave velocity, respectively, and ρ is the material's density. For the liquid MC the

DOI: 10.1021/acs.macromol.7b00270
Macromolecules XXXX, XXX, XXX−XXX

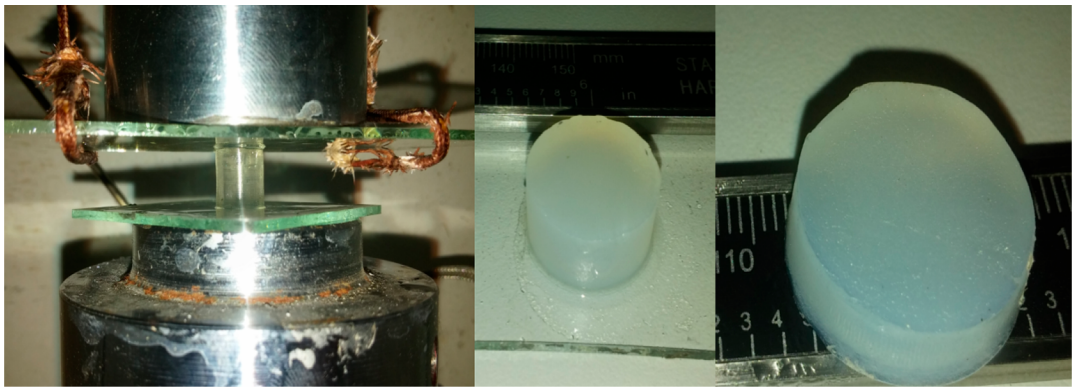

Figure 1. Gel samples before and after compression. From left to right: Glass plates used to reduce friction. MC-based hydrogels sample before the experiment. The same MC-based hydrogels sample after the experiment.

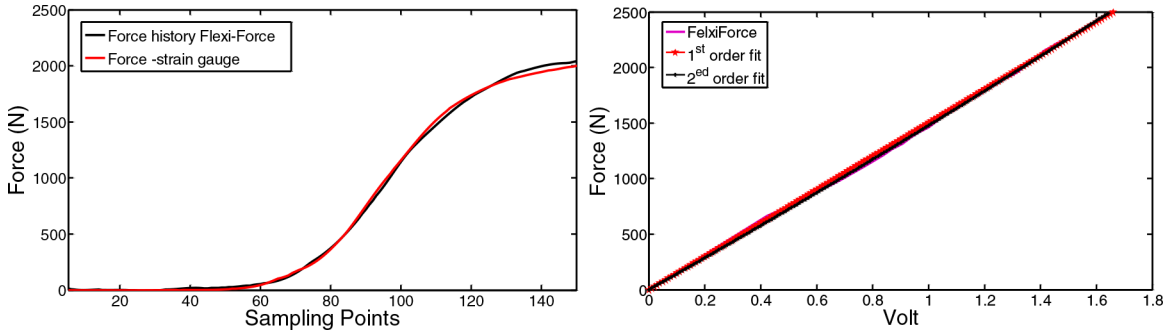

Figure 2. From left to right. Fitting between the forces measured with the strain gauges and those the force measured with FF sensors. Curve fitting for the volt to force ratio.

compressibility coefficient ($\beta = dV/dP$) can be calculated according to eq 3[69−72]

$$\beta = V_L^2 \rho \tag{3}$$

where dV is the change in volume and dP is the change in pressure.

Static Compression. Uniaxial quasi-static compression experiments were conducted using a screw-driven testing machine (Instron 4483), under displacement control, with a prescribed crosshead velocity of 3.6 mm/min. MC-based hydrogels gels were tested inside a temperature-controlled chamber at a temperature of 80 ± 3 °C. For high-resolution force measurements, a 500 N load cell was installed on the machine. During the experiments the force (F) and the displacement (ΔL) were recorded at 8 Hz frequency.

In order to minimize frictional effects and thus avoid barreling of the sample (see Figure 1), two custom glass plate adapters were installed on the conventional compression gigs.[44] Moreover, before each test, the glass plates were wetted with a few drops of water to reduce friction, achieving the sought-after effect.

Samples were cast into sealed glass vials with an internal diameter of 18 mm. They were then heated in the temperature control temperature (set at 80 °C) for 4 min to afford the gel state (nonequilibrated, this time period includes both heating and annealing). Immediately after this heating, the gel was then carefully extracted out of the vial and sliced to yield a cylindrical sample with nominal diameter and height of D_0 = 18 mm and L_0 = 8 mm, respectively (an ∼20 s procedure). Since it was noticed that even at strains of 0.8−0.9 no failure occurs, the experiments were deliberately terminated at strains of 0.5−0.7. Pictures of a sample before and after compression are presented in Figure 1.

The measured load−displacement curves were reduced into engineering stress−strain curves, where the engineering stress (σ_{eng}) was calculated as the applied load divided by the original cross-section area (A_0).

$$\sigma_{eng} = \frac{F}{A_0} \tag{4}$$

Hence, the engineering strain (ε_{eng}) was calculated as

$$\varepsilon_{eng} = \frac{\Delta L}{L_0} \tag{5}$$

where L_0 is the original specimen height and ΔL is the measured extension.

Dynamic Compression. The dynamic compression experiments were performed using a conventional 12.7 mm diameter Kolsky apparatus,[60] made of 7075-T6 aluminum-alloy bars, which were loaded at the far end of the incident bar with a projectile made of the same material. Once the striker hits the incident bar, a compression stress wave propagates along the incident bar until it reaches its end. At that point, the stress wave reaches the interface between the incident bar and the specimen. Here, part of the incident stress wave propagates through the specimen into the transmitted bar, while another part reflected back in the incident bar. The incident, reflected, and transmitted stress waves, ε_{inc}, ε_{ref}, and ε_{tra}, respectively, are measured by strain gauges (SG) and recorded using a Nicolet 440 digital oscilloscope. The displacements and the forces acting on each side of the specimen can usually be obtained from 1D wave propagation analysis.[73] The applied forces on each side of the specimen are calculated based on the measured strains and can thus be checked for dynamic force equilibrium.

$$F_1 = AE(\varepsilon_r + \varepsilon_i)$$
$$F_2 = AE(\varepsilon_t) \tag{6}$$

1D wave analysis based on SG measurements usually fits when the tested material has acoustic impedance close to the acoustic impedance of the Hopkinson bars.[61] For testing soft materials, such as gels, where the acoustic impedances of the specimen and the bars are very different, few modifications for the Kolsky apparatus can be

DOI: 10.1021/acs.macromol.7b00270
Macromolecules XXXX, XXX, XXX−XXX

found in the literature.[61,74−77] The modifications added to the compression Kolsky apparatus were performed according to the principles of previous work.[78]

- For low-amplitude force measurements, standard 201HT Flexi-force (FF) force sensors were placed on the edges of the Hopkinson's bar, so that the interfacial forces are measured directly and not through signal analysis.
- A pulse shaper,[61,79] consisting of soft paper mixed with a carefully measured amount of molybdenum disulfide grease, was inserted between the striker and the incident bar. The pulse shaper is used to increase the rise time of the loading pulse, thereby improving the specimen equilibrium due to lowered accelerations.[80] Because of the use of pulse shapers, the strain rate is not constant throughout the tests as it increases with strain to reach a peak value. The reported strain rates are the peak values.
- In order to ensure constant environmental temperature and humidity to 70 °C and 100%, respectively, a sealed heating chamber was designed and built.
- To validate the FF sensors' response, the volt to force relation was measured at the beginning and at the end of each experimental set by performing three shots without specimen between the Kolsky bars. The experimental force history was compared recorded signal on the two FF sensors. An example for force−volt comparison is shown in Figure 2.

In all the experiments, the area of the MC-based hydrogel specimens was in the range 9−16 mm^2, and the specimen thickness was in the range 2−4.5 mm. A representative photo of the modified Kolsky apparatus is shown in Figure 3.

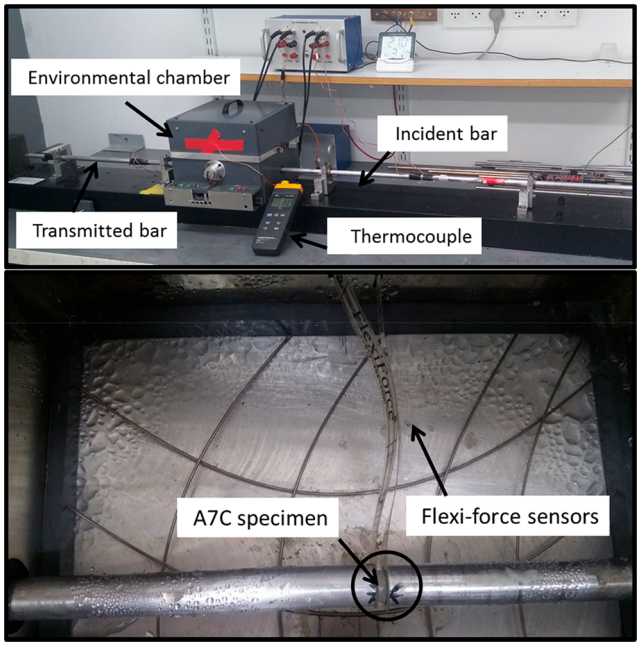

Figure 3. Upper: the modified Kolsky apparatus with the environmental chamber. Lower: **A7C** sample placed between the Kolsky bars with the Flexi-force sensors.

RESULTS AND DISCUSSION

Ultrasonic Characterization of Elastic Moduli. The longitudinal (V_L) and shear (V_T) wave speeds of the MC **A7C**-based hydrogel at a concentration of 56 g/L were measured at 14 and 80 °C as a solution and at the gel state, respectively. Since the velocity measurement itself has inherent statistical scatter, a large number of measurements (over 40 for V_L and above 10 for V_T) were performed. Moreover, the ultrasonic wave velocity of tap water and 20% ballistic gelatin 300 bloom were measured at room temperature in order to assess the ultrasonic measurement technique. The mean ultrasonic longitudinal wave velocity of measured water and ballistic gelatin were 1487 and 1577 m/s, respectively. Those results are in fine agreement with the velocities reported in the literature.[81,82] The measured longitudinal wave speeds of the **A7C**-based hydrogel at its liquid and solid-like state are shown in Figures 4a and 4b, respectively.

A summary of the ultrasonic measurements and the elastic moduli of the MC **A7C** at gel and liquid state is shown in Table 2.

The ultrasonic longitudinal velocity of the hydrogel in the liquid state is in proximity with those reported in the literature at the given range of temperature.[83] Moreover, the increase in the ultrasonic longitudinal velocity with increase in temperature fits the trend shown before for MC hydrogels and solution.[84,85]

Quasi-Static Compression. *Repeatability and Homogeneity.* Assessing repeatability and reproducibility of the experimental results was the first concern of this work. Because of the high temperature environment and the final manual slicing of the specimen, some variation in the measured flow stress may occur. In order to ensure the reliability of the obtained results, each type of experiment was performed 3−10 times. The repeatability of the flow stress measurements of **A7C**- and **A15C**-based hydrogels 56 g/L at 80 °C are illustrated in Figure 1S. The curves show small variations between samples and a transition from linear to nonlinear hardening at strains of 0.15 and 0.2 for the **A7C**- and **A15C**-based hydrogels, respectively. This trend is common in elastomers and other types of gels.[20,48,86−88]

With the aim of characterizing the spatial homogeneity of the sample, different portions of the same sample were tested separately. Since the cold aqueous MC solution may be stored for a few days before the experiment and is not stirred before measurement, it was important to rule out sedimentation of the polymer. Such a process might cause a strain gradient in the specimen, so that the upper part might be much weaker than the lower part.

For this purpose, four **A7C**-based hydrogel specimens were stored for 4 days at 4 °C, heated to 80 °C, and split into half. Each of these portions was tested separately (Figure 2S).

Figure 2S shows that the gel remains spatially homogeneous during the storage time, as no difference is observed in the stress−strain curves of the various tested specimens. Moreover, samples which were stored for 14 days at 4 °C exhibited similar flow stress to specimens with minimal storage time (12 h).

Temperature and Polymer Concentration. **A7C**- and **A15C**-based hydrogel samples at three different concentrations, 28, 44, and 56 g/L, were prepared and measured. Typical stress−strain curves of these samples with different concentration at a temperature of 80 °C are shown in Figure 5.

Figure 5 shows that the strength of the MC-based gel increases with increasing polymer concentration. For instance, at a strain of 0.5 the **A7C** sample with 28 g/L possesses a flow stress of ∼33 kPa; by doubling the concentration of MC in the sample, the flow stress at the same strain is increased by 10-fold to ∼328 kPa. Similarly, but to a lesser extent, **A15C**-based hydrogel with a concentration of 28 g/L, at a strain of 0.5, possesses a flow stress of ∼12 kPa, while **A15C**-based hydrogel with a concentration of 56 g/L possesses a flow stress of ∼60 kPa. As can be seen, for all concentrations examined **A7C**-based hydrogels consistently show higher flow stress than **A15C**-

DOI: 10.1021/acs.macromol.7b00270
Macromolecules XXXX, XXX, XXX−XXX

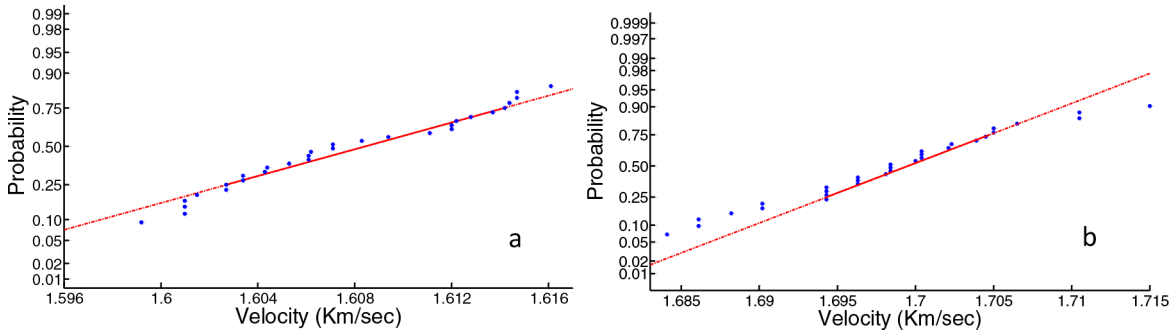

Figure 4. An approximation to normal distribution of the measured wave velocity of MC **A7C**-based hydrogel at a concentration of 56 g/L: (a) liquid state and (b) solid state.

Table 2. Summary of the Ultrasonic Measurements and the Elastic Moduli and the MC A7C-Based Hydrogels at Gel and Liquid State[a]

	longitudinal bulk velocity (m/s)	shear wave velocity (m/s)	Young's modulus E (GPa)	Poisson's ratio ν
gel 80 °C	1699 ± 10	1010 ± 5	2.45 ± (2.91 × 10^{-5})	0.227 ± 0.005
	longitudinal wave velocity (m/s)	shear wave velocity (m/s)		compressibility coefficient β (1/GPa)
liquid 14 °C	1607 ± 7			0.386 ± 0.003

[a]The deviations in the table are the standard deviations according to normal distribution fitting.

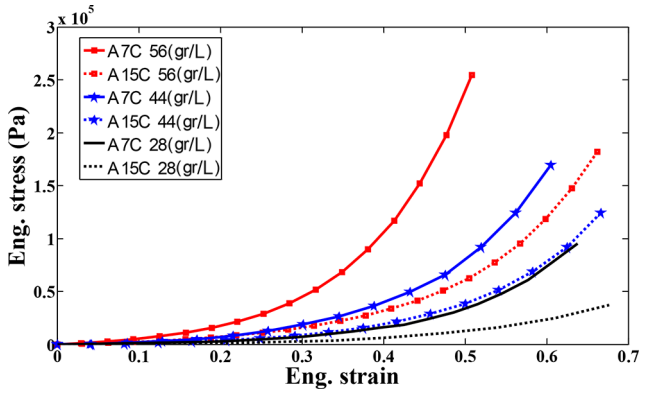

Figure 5. Quasi-static tests at strain rate of 7.5 × 10^{-3} s^{-1} at 80 °C. Engineering stress−strain curves of **A7C** and **A15C** MC gels at different MC concentrations: **A7C**, solid lines; **A15C**, dashed lines.

based hydrogels. This could be due to the average larger values of DS for the **A7C** type[89] and is not surprising as this MC is commercially intended for its higher strength compared to other MC gels.

Based on viscosity measurements, methyl cellulose hydrogels were reported to increase their strength with increase in polymer concentration.[90] Furthermore, G', and therefore E', has been reported to increase strongly with a scaling of more than square of the concentration for low-concentration MC hydrogels at 70 °C.[16] In light of these reports the correlation found here, based on compression tests, between concentration and rise in stiffness was expected. With higher content of polymer chains, including loci of interactions between them, more association sites are available and a denser 3D fibrilar network can form, over larger volumes of media. Such networks confer to the gel an increased ability to resist strain and therefore a higher flow stress.

Characterizing the influence of the temperature on the mechanical properties of our gels is essential since these properties change considerably on crossing the gelation temperature. Therefore, the mechanical response of a fixed selected gel concentration of 56 g/L was initially measured at the lowest temperature, that is, still above the T_g of the lowest-T_g sample (65 °C) as a reference. Then, additional samples were stabilized at temperatures of 80 and 100 °C and then tested. Typical flow curves of **A7C**- and **A15C**-based hydrogel samples are shown in Figure 6.

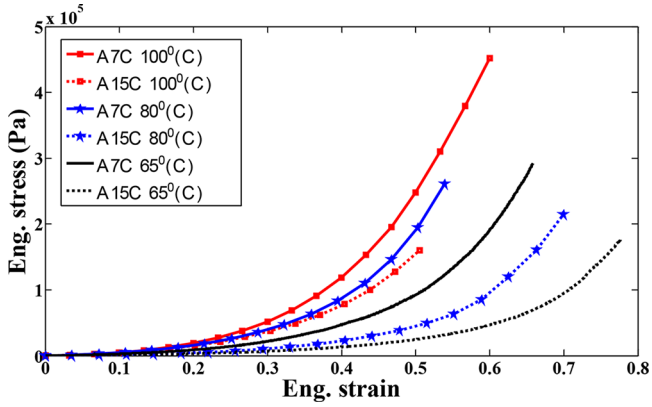

Figure 6. Quasi-static tests at a strain rate of 7.5 × 10^{-3} s^{-1}. Engineering stress−strain curves of **A7C** and **A15C** MC-based hydrogels (56 g/L) at different environmental temperatures. **A7C**, solid lines; **A15C**, dashed lines.

Figure 6 shows the uniqueness of the thermoreversible gelation phenomenon: the gels stiffen as the temperature increases. Interestingly, even at 65 °C, both gels exhibit reproducible, solid-like mechanical behavior. For example, at a strain of 0.5 the **A7C**-based hydrogel sample tested at 65 °C exhibits a flow stress of ∼92 kPa; by increasing the temperature to 100 °C, the stress reaches a value ∼247 kPa, which is about 2.5 times larger. **A15C**-based hydrogel exhibits an even larger hardening (6-fold). For a strain of 0.5 the flow stress of **A15C**-based hydrogel shifts from ∼24 kPa at 65 °C to ∼150 kPa at 100 °C.

DOI: 10.1021/acs.macromol.7b00270
Macromolecules XXXX, XXX, XXX−XXX

In order to verify that this stiffening with increased temperature is not unique only to the gel with the specific concentration described above, MC gels with another polymer concentration of 44 g/L were also prepared and tested. Flow stress curves of **A7C**-based hydrogel at this concentration compared to the 56 g/L samples are shown in Figure 7 as a function of the temperature.

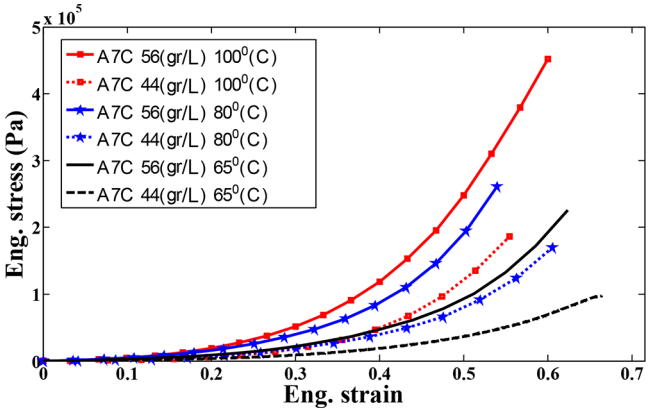

Figure 7. Quasi-static tests at strain rate 7.5×10^{-3} (1/s). Engineering stress−strain curves of **A7C** sample at two different concentrations, at different environmental temperatures. 56 g/L, solid lines; 44 g/L, dashed lines.

The results in Figure 7 imply that temperature-caused increase of gel flow stress occurs over a range of concentrations of MC polymer in the gel.

To our knowledge, this is the first demonstration of MC gel-state mechanical stiffening as a function of strain, by heating beyond the gelation point, as determined by straightforward monotonic compression tests, which complements the previous report.[20]

MC has been reported in the literature to increase its viscosity with increase in temperature, including beyond the gelation point.[13,33] Since it has been shown that the mechanical and optical manifestations of gelation are concurrent,[62] at all three temperatures measured the samples have already undergone gelation (they are all opaque). Percolation models,[87,91−93] often used to explain the transition from liquid to solid, also do not explain increased stress flow properties with further heating of our "solid".

Rheological experiments have shown that G', as a function of angular frequency up to values of 100 (rad/s), reaches a plateau at around 65−70 °C in the second stage of heat-induced gelation, corresponding to the formation of a strong gel.[16] A more recent investigation reveals that the gels' plateau storage modulus, as a function of applied rheological stress, increases (from certain stresses upward) with temperature.[20] This remarkable behavior occurs only above T_g and is attributed to the gel's fibrillar structure, distinct from other soft gels composed of entangled flexible polymers. Our novel findings therefore complement these previous results and provide additional evidence that the gel's response to heating is not similar to those of the majority of other solids, either crystalline or classic amorphous (such as glass).

Heat applied to most known solids causes increased vibration of their components and weakening of their bonds (whether intermolecular in molecular solids or covalent/ionic in atomic solids), leading to decreased flow stress. However, MC hydrogels exhibit just the opposite behavior (at least in the examined temperature range). Since care was taken to prevent loss of water, increasing polymer concentration through solvent loss from the gel is an unlikely explanation of our results. While the underlying cause of this phenomenon requires further study, we propose that the literature-offered mechanisms leading to gelation from the liquid phase continue to be active and relevant in the gel phase as well: upon heating, association between more polymer chains continues to occur,[94] shedding of structured solvent, formation of more fibrils and their growth, increasing network density, and in turn leading to higher stiffness. A recent inspiring work by Guo et al. presents both the engineering and the trait exploration of a hydrogel based on two functional components: cross-linked PNIPAm with hydrophilic side chains.[95] The former maintains its LCST feature and phase-separates with increased temperature, while the latter maintains water within the network and therefore prevents large volume changes upon this transition. As a result of these features, this hydrogel presents thermoresponsive toughening (increasing with temperature up to 60 °C), as examined by tensile tests. However, as the examined hydrogels in this work are based on a different polymer with a different gelation mechanism, we are careful at this stage about drawing parallel conclusions on the microscopic factors leading to toughening in our case.

Strain Rate Sensitivity. Hydrogels are known to exhibit strain rate sensitivity;[19,96] i.e., the flow stress response depends on the rate of the strain applied to it. Since this is a common mechanical property of soft, viscous materials, we expected to find it also for our MC-based hydrogel samples. In this work we focus on the gel state, and its response to compression loading over a wide range of loading (strain) rates and for large strains. First, in order to examine whether the **A7C** gel is strain rate sensitive within the quasi-static loading regime, the crosshead velocity of the Instron loading frame was varied to cover a range of nominal strain rates between 7.5×10^{-3} and 4×10^{-1} s^{-1}. Typical flow stress curves of **A7C** 56 g/L hydrogel samples tested at 80 °C are shown in Figure 8 for various strain rates.

According to Figure 8, there is no evidence for strain rate sensitivity in the investigated range of strain rates. These results were rather surprising, since many soft gels tend to exhibit strain rate sensitivity.[76,97]

Dynamic Compression. Experiments at much higher strain rates, ∼1500 s^{-1}, were conducted using the split

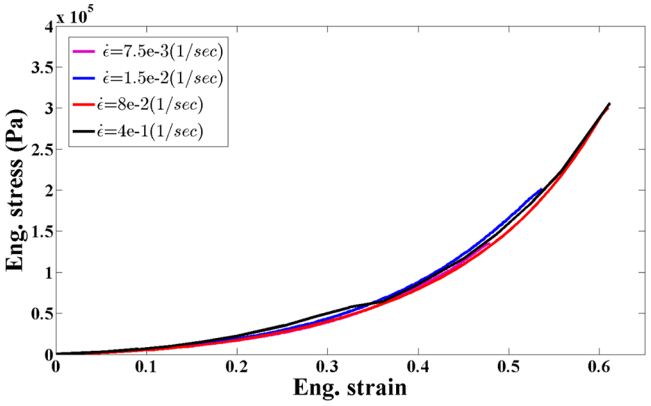

Figure 8. Quasi-static tests. Engineering stress−strain curves of MC **A7C**-based gel samples (56 g/L) at different strain rates within the quasi-static loading regime at 80 °C.

DOI: 10.1021/acs.macromol.7b00270
Macromolecules XXXX, XXX, XXX−XXX

Hopkinson pressure bar (Kolsky apparatus).[60] As extensively shown in the literature,[80,98] dynamic force equilibrium has to be verified before the measured signals from the strain gauges can be converted into stress−strain curves. In contrast to the common three signals analysis,[73] in our experimental setup, the dynamic force equilibrium was measured directly with the FF gauges by comparing the forces on both sides of the samples. While in conventional Hopkinson experiments the forces' amplitude lies in the range of 15 000−40 000 N, in our experimental setup the measured forces were in the range of 1−12 N, which is quite unusual for this kind of test. A typical dynamic force equilibrium is shown in Figure 9 for an **A7C** gel sample.

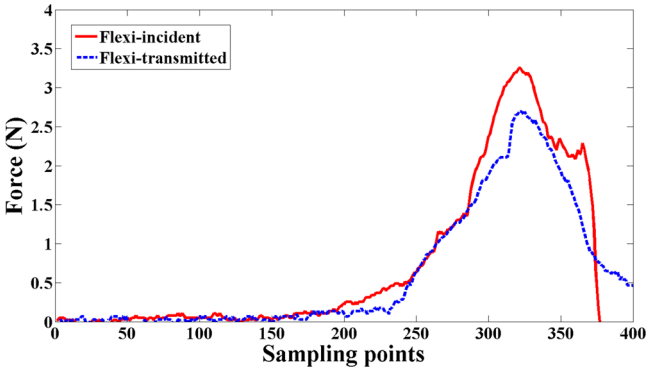

Figure 9. Dynamic test. Representative F_in and F_out histories as a measure of the dynamic force equilibrium. Note that the forces' amplitude may change according to the specimen's diamensions and the strain rate.

The force histories shown in Figure 9 indicate satisfactory dynamic force equilibrium. Therefore, the strain can be reliably calculated using the reflected signal ε_r. In a few cases where a satisfactory state of dynamic equilibrium was not achieved (due to the gel's acoustic impedance and high attenuation), the stress−strain curves were compared to experiments showing satisfactory dynamic force equilibrium in order to assess a good fit.

Representative true stress−true strain curves of **A7C** gel samples from split Hopkinson experiments, where the maximum strain rates were in the range of 1000−1600 1/s at 70 °C, are shown in Figure 10.

Similarly to the quasi-static compression experiments, the true stress−strain curves also exhibit repeatable behavior under dynamic loading. For all the characterized flow stress curves there is a mild hardening up to a strain of approximately 0.05, and from this value on, the MC gels stiffens (hardens) rapidly, until the specimen fails. In order to examine the strain rate sensitivity of the **A7C**-based hydrogel in a qualitative manner, we compared the dynamic and quasi-static flow curves as shown in Figure 11.

The curves in Figure 11 show a significant increase in the gel's flow stress (×10−20) when submitted to dynamic loading at the range of 10^3 1/s in comparison to the quasi-static loading. Studies reported in the literature, based on Kolsky bar measurements of other soft gels such as 10% and 20% ballistic gelatin at various bloom strengths, show only moderate increase in the gels' flow stress (×2−3).[78,99]

Rheology experiments on MC solutions have shown it to behave as a shear thinning fluid,[27,29,90] meaning that with higher shear rates the mechanical resistance of the fluid to flow

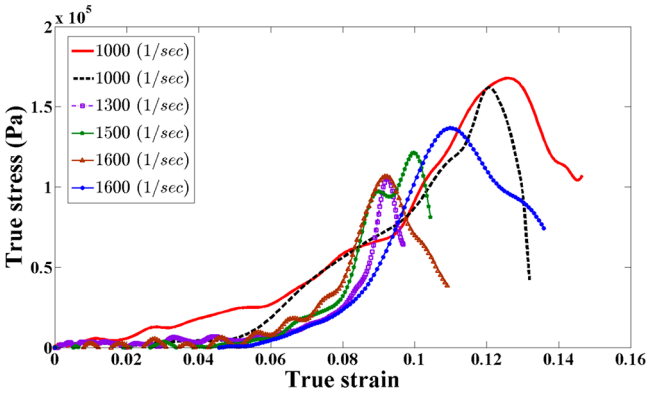

Figure 10. Dynamic compression true stress−true strain curves of **A7C**-based hydrogel samples (56 g/L) at 70 °C. Note the span (scatter) of failure strains for tests carried out at relatively similar strain rates.

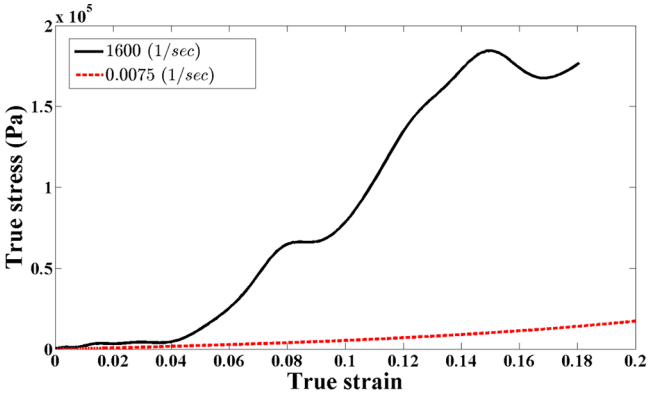

Figure 11. Comparison between flow curves of **A7C**-based hydrogel submitted to dynamic and static compression.

decreases. Furthermore, MC solutions undergoing shear stresses in a high pressure (20−350 MPa) homogenizer have been reported to undergo irreversible degradation and intrinsic viscosity reduction.[100] As mentioned in the Introduction, a recent report investigating the characteristics of the gel state discusses a transition to shear thickening behavior upon gelation.[20] Since one cannot establish a direct correlation between the small strain oscillatory behavior of a material and its behavior at high rate and large strains, our results are novel in showing that MC gels harden considerably under a higher rate of compression loading. A tentative explanation of the difference of behavior between the shear thinning in the MC at the liquid state to the compression of the solid gel is the higher restriction of movement of the polymer chains and their larger macromolecular structures such as the previously reported fibrils in nematic phases.[28] If so, these structures could provide the resistance to the compressive forces at the examined time scales, whereas on slower rates these structures have sufficient time to reorganize and shift to accommodate the new pressures.

The mechanical resistance to dynamic compression is also accompanied by a large reduction of ductility to failure, from over 70% (static) to less than 20% (dynamic), with a wide scatter, as illustrated in Figure 11. A possible explanation for the reduced dynamic ductility could be related to characteristic times for water diffusion in/out of the network (poroelasticity); however, this point requires further confirmation. In addition, this finding could support the possibility presented above

DOI: 10.1021/acs.macromol.7b00270
Macromolecules XXXX, XXX, XXX−XXX

regarding macromolecular structures that fail to spatially reorganize in the examined time scales. Finally, the observed scatter in ductility to failure may be related to submicroscopic flaws that could not be resolved by optical means.

CONCLUSIONS

We report here on the large strain mechanical properties of the gels of MC types **A7C** and **A15C**. This solid is unique in that it is the result of thermoreversible gelation and as such has characteristics different than that of most other hydrogels. Additionally, its recently discovered fibrillar structure sets it apart from other soft gels composed of flexible entangled polymers. These two distinct traits arouse the scientific interest to explore its ensuing mechanical properties. Our extensive mechanical characterization, which includes ultrasonic, quasi-static, and dynamic compression with Kolsky bars, was challenging due to the soft nature of this material.

For MC **A7C** 56 g/L at solid and liquid state we found a Young's modulus value of 2.45 ± (2.91 × 10^{-5}) GPa, a Poisson's ratio of 0.227 ± 0.005, and a compressibility coefficient of 0.386 ± 0.003 GPa^{-1}.

Quasi-static compression experiments revealed some interesting phenomena: The first is a correspondence of flow stress with concentration of the polymer. Second, heating beyond the gelation point leads to an increasing stiffness of the heated gel. The gel can withstand higher mechanical load at higher temperatures. We presume that this is due to the underlying mechanisms offered previously for the gelation continuing to take place as the gel is heated. We view this as a manifestation of this material's thermoreversible gelation property, since other solids normally soften when heated.

After observing a lack of strain rate sensitivity for the MC gel in the quasi-static experiments, dynamic compression showed remarkable strain rate sensitivity in the dynamic compared to the quasi-static loading regime. The gels' stiffening in the dynamic, compared to the quasi-static loading regime, is found to be 10−20-fold. This value is considerably higher than for other soft material gels we are familiar with. The dramatic increase in dynamic strength is accompanied by a significant reduction in the dynamic ductility to failure of the gel.

The methods developed and presented in this paper could be used to perform mechanical studies on other very soft materials. Furthermore, the values and characteristics reported herein could be beneficial for further development of applications of these commonly used materials.

ASSOCIATED CONTENT

Supporting Information

The Supporting Information is available free of charge on the ACS Publications website at DOI: 10.1021/acs.macromol.7b00270.

Figures 1S and 2S (PDF)

AUTHOR INFORMATION

Corresponding Author

*E-mail Y.rotbaum@gmail.com.

ORCID

Yonatan Rotbaum: 0000-0003-1139-2380

Notes

The authors declare no competing financial interest.

ACKNOWLEDGMENTS

This research is supported by the Technion's Center for Security Science and Technology, Grant 2020951. We thank DOW Chemical Company for the donation of the **A7C** MC sample.

REFERENCES

(1) Borzacchiello, A.; Ambrosio, L. *Hydrogels: Biological Properties and Applications*; Springer-Verlag: Berlin, 2009.

(2) Chang, C.; Zhang, L. Cellulose-based hydrogels: present status and application prospects. *Carbohydr. Polym.* **2011**, *84* (1), 40−53.

(3) Serra, M. Adaptable skin-hydrogel gives wetsuit protection. *Smart Mater. Bull.* **2002**, *8*, 7−8.

(4) Richter, A.; Paschew, G.; Klatt, S.; Lienig, J.; Arndt, K.-F.; Adler, H.-J. P. Review on hydrogel-based pH sensors and microsensors. *Sensors* **2008**, *8* (1), 561−581.

(5) Yahia, L.; Chirani, N.; Gritsch, L.; Motta, F. L. History and Applications of Hydrogels. *J. Biomed. Sci.* **2015**.10.4172/2254-609X.100013.

(6) Ahmed, E. M. Hydrogel: Preparation, characterization, and applications: A review. *Journal of advanced research* **2015**, *6* (2), 105−121.

(7) Peppas, N. A.; Ottenbrite, R. M.; Park, K.; Okano, T. *Biomedical Applications of Hydrogels Handbook*; Springer Science & Business Media: 2010.

(8) Nasatto, P. L.; Pignon, F.; Silveira, J. L.; Duarte, M. E. R.; Noseda, M. D.; Rinaudo, M. Methylcellulose, a cellulose derivative with original physical properties and extended applications. *Polymers* **2015**, *7* (5), 777−803.

(9) Schupper, N.; Shnerb, N. M. Inverse melting and inverse freezing: A spin model. *Phys. Rev. E* **2005**, *72* (4), 046107.

(10) Schild, H. G. Poly (N-isopropylacrylamide): experiment, theory and application. *Prog. Polym. Sci.* **1992**, *17* (2), 163−249.

(11) Heskins, M.; Guillet, J. E. Solution properties of poly (N-isopropylacrylamide). *J. Macromol. Sci., Chem.* **1968**, *2* (8), 1441−1455.

(12) Adden, R.; Anderson, W. H.; Huebner, B.; Knarr, M. Methods and compositions for inducing satiety. Google Patents, 2014.

(13) Hirrien, M.; Chevillard, C.; Desbrieres, J.; Axelos, M.; Rinaudo, M. Thermogelation of methylcelluloses: new evidence for understanding the gelation mechanism. *Polymer* **1998**, *39* (25), 6251−6259.

(14) Desbrieres, J.; Hirrien, M.; Rinaudo, M. A calorimetric study of methylcellulose gelation. *Carbohydr. Polym.* **1998**, *37* (2), 145−152.

(15) Li, L.; Thangamathesvaran, P.; Yue, C.; Tam, K.; Hu, X.; Lam, Y. Gel network structure of methylcellulose in water. *Langmuir* **2001**, *17* (26), 8062−8068.

(16) Kobayashi, K.; Huang, C.-i.; Lodge, T. P. Thermoreversible gelation of aqueous methylcellulose solutions. *Macromolecules* **1999**, *32* (21), 7070−7077.

(17) Sarkar, N. Kinetics of thermal gelation of methylcellulose and hydroxypropylmethylcellulose in aqueous solutions. *Carbohydr. Polym.* **1995**, *26* (3), 195−203.

(18) Herraez-Dominguez, J.; de Leon, F. G. G.; Diez-Sales, O.; Herráez-Domínguez, M. Rheological characterization of two viscosity grades of methylcellulose: an approach to the modeling of the thixotropic behaviour. *Colloid Polym. Sci.* **2005**, *284* (1), 86−91.

(19) Kundu, M.; Mallapragada, S.; Larock, R.; Kundu, P. Rheological properties of methylcellulose aqueous gels under dynamic compression: Frequency sweep and validity of scaling law. *J. Appl. Polym. Sci.* **2010**, *117* (4), 2436−2443.

(20) McAllister, J. W.; Lott, J. R.; Schmidt, P. W.; Sammler, R. L.; Bates, F. S.; Lodge, T. P. Linear and nonlinear rheological behavior of fibrillar methylcellulose hydrogels. *ACS Macro Lett.* **2015**, *4* (5), 538−542.

(21) Wang, Q.; Li, L. Effects of molecular weight on thermoreversible gelation and gel elasticity of methylcellulose in aqueous solution. *Carbohydr. Polym.* **2005**, *62* (3), 232−238.

DOI: 10.1021/acs.macromol.7b00270
Macromolecules XXXX, XXX, XXX−XXX

(22) Sarkar, N. Thermal gelation properties of methyl and hydroxypropyl methylcellulose. *J. Appl. Polym. Sci.* **1979**, *24* (4), 1073−1087.
(23) Kundu, P.; Kundu, M. Effect of salts and surfactant and their doses on the gelation of extremely dilute solutions of methyl cellulose. *Polymer* **2001**, *42* (5), 2015−2020.
(24) Xu, Y.; Li, L.; Zheng, P.; Lam, Y. C.; Hu, X. Controllable gelation of methylcellulose by a salt mixture. *Langmuir* **2004**, *20* (15), 6134−6138.
(25) Xu, Y.; Li, L. Thermoreversible and salt-sensitive turbidity of methylcellulose in aqueous solution. *Polymer* **2005**, *46* (18), 7410−7417.
(26) Knarr, M.; Bayer, R. The shear dependence of the methylcellulose gelation phenomena in aqueous solution and in ceramic paste. *Carbohydr. Polym.* **2014**, *111*, 80−88.
(27) Haque, A.; Morris, E. R. Thermogelation of methylcellulose. Part I: molecular structures and processes. *Carbohydr. Polym.* **1993**, *22* (3), 161−173.
(28) McAllister, J. W.; Schmidt, P. W.; Dorfman, K. D.; Lodge, T. P.; Bates, F. S. Thermodynamics of Aqueous Methylcellulose Solutions. *Macromolecules* **2015**, *48* (19), 7205−7215.
(29) Li, L. Thermal gelation of methylcellulose in water: scaling and thermoreversibility. *Macromolecules* **2002**, *35* (15), 5990−5998.
(30) Li, L.; Shan, H.; Yue, C.; Lam, Y.; Tam, K.; Hu, X. Thermally induced association and dissociation of methylcellulose in aqueous solutions. *Langmuir* **2002**, *18* (20), 7291−7298.
(31) Plazanet, M.; Dean, M.; Merlini, M.; Huller, A.; Emerich, H.; Meneghini, C.; Johnson, M.; Trommsdorff, H. Crystallization on heating and complex phase behavior of alpha-cyclodextrin solutions. *J. Chem. Phys.* **2006**, *125* (15), 154504.
(32) Lott, J. R.; McAllister, J. W.; Arvidson, S. A.; Bates, F. S.; Lodge, T. P. Fibrillar structure of methylcellulose hydrogels. *Biomacromolecules* **2013**, *14* (8), 2484−2488.
(33) Bodvik, R.; Dedinaite, A.; Karlson, L.; Bergström, M.; Bäverbäck, P.; Pedersen, J. S.; Edwards, K.; Karlsson, G.; Varga, I.; Claesson, P. M. Aggregation and network formation of aqueous methylcellulose and hydroxypropylmethylcellulose solutions. *Colloids Surf., A* **2010**, *354* (1), 162−171.
(34) Kong, M.; Saha Dalal, I.; Li, G.; Larson, R. G. Systematic coarse-graining of the dynamics of self-attractive semiflexible polymers. *Macromolecules* **2014**, *47* (4), 1494−1502.
(35) Huang, W.; Ramesh, R.; Jha, P. K.; Larson, R. G. A systematic coarse-grained model for methylcellulose polymers: Spontaneous ring formation at elevated temperature. *Macromolecules* **2016**, *49* (4), 1490−1503.
(36) Ginzburg, V. V.; Sammler, R. L.; Huang, W.; Larson, R. G. Anisotropic self-assembly and gelation in aqueous methylcellulose—theory and modeling. *J. Polym. Sci., Part B: Polym. Phys.* **2016**, *54* (16), 1624−1636.
(37) Patel, T. R.; Morris, G. A.; de la Torre, J. G.; Ortega, A.; Mischnick, P.; Harding, S. E. Molecular flexibility of methylcelluloses of differing degree of substitution by combined sedimentation and viscosity analysis. *Macromol. Biosci.* **2008**, *8* (12), 1108−1115.
(38) Pavlov, G.; Michailova, N.; Tarabukina, E.; Korneeva, E. Velocity sedimentation of water-soluble methyl cellulose. In *Analytical Ultracentrifugation*; Springer: 1995; pp 109−113.
(39) Chen, W. W. Experimental methods for characterizing dynamic response of soft materials. *Journal of Dynamic Behavior of Materials* **2016**, *2* (1), 2−14.
(40) Miller, K.; Chinzei, K. Mechanical properties of brain tissue in tension. *J. Biomech.* **2002**, *35* (4), 483−490.
(41) Sun, W.; Sacks, M. S.; Scott, M. J. Effects of boundary conditions on the estimation of the planar biaxial mechanical properties of soft tissues. *J. Biomech. Eng.* **2005**, *127* (4), 709−715.
(42) Saraf, H.; Ramesh, K.; Lennon, A.; Merkle, A.; Roberts, J. Mechanical properties of soft human tissues under dynamic loading. *J. Biomech.* **2007**, *40* (9), 1960−1967.
(43) Knarr, M.; Adden, R.; Anderson, W. K.; Hübner-Keese, B. Characterization of in-vitro gel performance of novel MC with respect to the suitability for satiety applications. *Food Hydrocolloids* **2012**, *29* (2), 317−325.
(44) Miquelard-Garnier, G.; Creton, C.; Hourdet, D. Strain induced clustering in polyelectrolyte hydrogels. *Soft Matter* **2008**, *4* (5), 1011−1023.
(45) Webber, R. E.; Creton, C.; Brown, H. R.; Gong, J. P. Large strain hysteresis and mullins effect of tough double-network hydrogels. *Macromolecules* **2007**, *40* (8), 2919−2927.
(46) White, J. C.; Saffer, E. M.; Bhatia, S. R. Alginate/PEO-PPO-PEO composite hydrogels with thermally-active plasticity. *Biomacromolecules* **2013**, *14* (12), 4456−4464.
(47) Buyanov, A.; Gofman, I.; Revel'skaya, L.; Khripunov, A.; Tkachenko, A. Anisotropic swelling and mechanical behavior of composite bacterial cellulose−poly (acrylamide or acrylamide−sodium acrylate) hydrogels. *Journal of the Mechanical Behavior of Biomedical Materials* **2010**, *3* (1), 102−111.
(48) Stammen, J. A.; Williams, S.; Ku, D. N.; Guldberg, R. E. Mechanical properties of a novel PVA hydrogel in shear and unconfined compression. *Biomaterials* **2001**, *22* (8), 799−806.
(49) Lee, S.-Y.; Pereira, B. P.; Yusof, N.; Selvaratnam, L.; Yu, Z.; Abbas, A.; Kamarul, T. Unconfined compression properties of a porous poly (vinyl alcohol)−chitosan-based hydrogel after hydration. *Acta Biomater.* **2009**, *5* (6), 1919−1925.
(50) Chau, M.; De France, K. J.; Kopera, B.; Machado, V. R.; Rosenfeldt, S.; Reyes, L.; Chan, K. J.; Förster, S.; Cranston, E. D.; Hoare, T. Composite hydrogels with tunable anisotropic morphologies and mechanical properties. *Chem. Mater.* **2016**, *28* (10), 3406−3415.
(51) Chang, C.; Peng, J.; Zhang, L.; Pang, D.-W. Strongly fluorescent hydrogels with quantum dots embedded in cellulose matrices. *J. Mater. Chem.* **2009**, *19* (41), 7771−7776.
(52) Duan, J.; Zhang, X.; Jiang, J.; Han, C.; Yang, J.; Liu, L.; Lan, H.; Huang, D. The synthesis of a novel cellulose physical gel. *J. Nanomater.* **2014**, *2014*, 1−7.
(53) Roy, N.; Saha, N.; Kitano, T.; Saha, P. Development and characterization of novel medicated hydrogels for wound dressing. *Soft Mater.* **2010**, *8* (2), 130−148.
(54) Ivanov, C.; Popa, M.; Ivanov, M.; Popa, A. Synthesis of poly (vinyl alcohol): methyl cellulose hydrogel as possible scaffolds in tissue engineering. *J. Optoelectron. Adv. Mater.* **2007**, *9* (11), 3440−3444.
(55) Negim, E.; Nurpeissova, Z. A.; Mangazbayeva, R.; Khatib, J.; Williams, C.; Mun, G. Effect of pH on the physico-mechanical properties and miscibility of methyl cellulose/poly (acrylic acid) blends. *Carbohydr. Polym.* **2014**, *101*, 415−422.
(56) Rajabi-Siahboomi, A.; Nokhodchi, A. Compression properties of methylcellulose and hydroxypropylmethylcellulose polymers. *Pharm. Pharmacol. Commun.* **1999**, *5* (2), 67−71.
(57) Park, H. J.; Weller, C.; Vergano, P.; Testin, R. Permeability and mechanical properties of cellulose-based edible films. *J. Food Sci.* **1993**, *58* (6), 1361−1364.
(58) Rimdusit, S.; Jingjid, S.; Damrongsakkul, S.; Tiptipakorn, S.; Takeichi, T. Biodegradability and property characterizations of methyl cellulose: effect of nanocompositing and chemical crosslinking. *Carbohydr. Polym.* **2008**, *72* (3), 444−455.
(59) Zhang, Y.; Gao, C.; Li, X.; Xu, C.; Zhang, Y.; Sun, Z.; Liu, Y.; Gao, J. Thermosensitive methyl cellulose-based injectable hydrogels for post-operation anti-adhesion. *Carbohydr. Polym.* **2014**, *101*, 171−178.
(60) Kolsky, H. *An Investigation of the Mechanical Properties of Materials at Very High Rates of Loading*; IOP Publishing: 1949; Vol. *62*, p 676.
(61) Chen, W.; Song, B. *Split Hopkinson (Kolsky) Bar: Design, Testing and Applications*; Springer: 2011.
(62) Arvidson, S.; Lott, J.; McAllister, J.; Zhang, J.; Bates, F.; Lodge, T.; Sammler, R.; Li, Y.; Brackhagen, M. Interplay of phase separation and thermoreversible gelation in aqueous methylcellulose solutions. *Macromolecules* **2013**, *46* (1), 300−309.
(63) Rose, J. L. *Ultrasonic Waves in Solid Media*; Cambridge University Press: 2004.

DOI: 10.1021/acs.macromol.7b00270
Macromolecules XXXX, XXX, XXX−XXX

(64) Chen, C.-h. *Ultrasonic and Advanced Methods for Nondestructive Testing and Material Characterization*; World Scientific: 2007.
(65) Blitz, J. Ultrasonics: methods and applications, 1971.
(66) Hahn, S. L. *Hilbert Transforms in Signal Processing*; Artech House: 1996.
(67) Polking, J. C. *MATLAB Manual, Ordinary Differential Equations*; Prentice Hall PTR: 1995.
(68) Cheeke, J. D. N. *Fundamentals and Applications of Ultrasonic Waves*; CRC Press: 2012.
(69) Jacobson, B. Ultrasonic velocity in liquids and liquid mixtures. *J. Chem. Phys.* **1952**, *20* (5), 927−928.
(70) Pinkerton, J. The absorption of ultrasonic waves in liquids and its relation to molecular constitution. *Proc. Phys. Soc., London, Sect. B* **1949**, *62* (2), 129.
(71) Chhapgar, A. Ultrasonic Velocities in Solutions and Mixtures. *J. Acoust. Soc. Am.* **1953**, *25* (4), 794−795.
(72) Deshpande, D.; Bhatgadde, L. Sound velocities, adiabatic compressibilities, and free volumes in aniline solutions. *J. Phys. Chem.* **1968**, *72* (1), 261−266.
(73) Lifshitz, J.; Leber, H. Data processing in the split Hopkinson pressure bar tests. *International Journal of Impact Engineering* **1994**, *15* (6), 723−733.
(74) Chen, W.; Lu, F.; Zhou, B. A quartz-crystal-embedded split Hopkinson pressure bar for soft materials. *Exp. Mech.* **2000**, *40* (1), 1−6.
(75) Song, B.; Chen, W. Split Hopkinson pressure bar techniques for characterizing soft materials. *Lat. Am. J. Solids Struct.* **2005**, *2* (2), 113−152.
(76) Kwon, J.; Subhash, G. Compressive strain rate sensitivity of ballistic gelatin. *J. Biomech.* **2010**, *43* (3), 420−425.
(77) Benatar, A.; Rittel, D.; Yarin, A. Theoretical and experimental analysis of longitudinal wave propagation in cylindrical viscoelastic rods. *J. Mech. Phys. Solids* **2003**, *51* (8), 1413−1431.
(78) Richler, D.; Rittel, D. On the Testing of the Dynamic Mechanical Properties of Soft Gelatins. *Exp. Mech.* **2014**, *54* (5), 805−815.
(79) Frew, D.; Forrestal, M. J.; Chen, W. Pulse shaping techniques for testing brittle materials with a split Hopkinson pressure bar. *Exp. Mech.* **2002**, *42* (1), 93−106.
(80) Davies, E.; Hunter, S. The dynamic compression testing of solids by the method of the split Hopkinson pressure bar. *J. Mech. Phys. Solids* **1963**, *11* (3), 155−179.
(81) Shepherd, C.; Appleby-Thomas, G.; Hazell, P.; Allsop, D.; Elert, M.; Furnish, M. D.; Anderson, W. W.; Proud, W. G.; Butler, W. T. In *The Dynamic Behaviour of Ballistic Gelatin*; AIP Conference Proceedings, 2009; AIP: 2009; pp 1399−1402.
(82) Aihaiti, M.; Hemley, R. J. *Equation of State of Ballistic Gelatin (II)*; DTIC Document: 2011.
(83) Matsuoka, T.; Maebayahshi, M.; Nagayama, Y.; Koda, S.; Nomura, H. Measurement of ultrasonic velocity of hydrogels in low-temperature region. *Japanese journal of applied physics* **2003**, *42* (5S), 2944.
(84) Jayaraju, J.; Raviprakash, S.; Keshavayya, J.; Rai, S. Miscibility studies on chitosan/hydroxypropylmethyl cellulose blend in solution by viscosity, ultrasonic velocity, density, and refractive index methods. *J. Appl. Polym. Sci.* **2006**, *102* (3), 2738−2742.
(85) Matsuoka, T.; Fujimura, S.; Nakamura, Y.; Koda, S.; Nomura, H. Effect of molecular weight and degree of substitution on the shear modulus of methyl cellulose gel by means of surface wave method. *Japanese journal of applied physics* **2002**, *41* (5S), 3181.
(86) Wang, X.; Wang, H.; Brown, H. R. Jellyfish gel and its hybrid hydrogels with high mechanical strength. *Soft Matter* **2011**, *7* (1), 211−219.
(87) Djabourov, M. Gelation—A review. *Polym. Int.* **1991**, *25* (3), 135−143.
(88) Woignier, T.; Despetis, F.; Alaoui, A.; Etienne, P.; Phalippou, J. Mechanical properties of gel-derived materials. *J. Sol-Gel Sci. Technol.* **2000**, *19* (1−3), 163−169.
(89) Reibert, K. C.; Conklin, J. R. Process for making cellulose ether having enhanced gel strength. Google Patents, 2001.
(90) Ethers, M. C. *Technical Handbook*; Dow Chemical Company: Midland, MI,1997.
(91) Stauffer, D.; Aharony, A. *Introduction to Percolation Theory*; CRC Press: 1994.
(92) Shi, Y.; Falk, M. L. Strain localization and percolation of stable structure in amorphous solids. *Phys. Rev. Lett.* **2005**, *95* (9), 095502.
(93) Adam, M.; Delsanti, M.; Durand, D.; Hild, G.; Munch, J. Mechanical properties near gelation threshold, comparison with classical and 3d percolation theories. *Pure Appl. Chem.* **1981**, *53* (8), 1489−1494.
(94) Huang, W.; Dalal, I. S.; Larson, R. G. Analysis of solvation and gelation behavior of methylcellulose using atomistic molecular dynamics simulations. *J. Phys. Chem. B* **2014**, *118* (48), 13992−14008.
(95) Guo, H.; Sanson, N.; Hourdet, D.; Marcellan, A. Thermoresponsive Toughening with Crack Bifurcation in Phase-Separated Hydrogels under Isochoric Conditions. *Adv. Mater.* **2016**, *28* (28), 5857−5864.
(96) Aranda-Iglesias, D.; Vadillo, G.; Rodríguez-Martínez, J.; Volokh, K. Modeling deformation and failure of elastomers at high strain rates. *Mech. Mater.* **2016**, *104*, 85.
(97) Salisbury, C.; Cronin, D. Mechanical properties of ballistic gelatin at high deformation rates. *Exp. Mech.* **2009**, *49* (6), 829−840.
(98) Rotbaum, Y.; Rittel, D. Is There An Optimal Gauge Length for Dynamic Tensile Specimens? *Exp. Mech.* **2014**, *54* (7), 1205.
(99) Moy, P.; Weerasooriya, T.; Gunnarsson, C. A. In Tensile deformation of ballistic gelatin as a function of loading rate, Proceedings of the XIth International Congress and Exposition, June 2008.
(100) Floury, J.; Desrumaux, A.; Axelos, M. A.; Legrand, J. Degradation of methylcellulose during ultra-high pressure homogenisation. *Food Hydrocolloids* **2002**, *16* (1), 47−53.

DOI: 10.1021/acs.macromol.7b00270
Macromolecules XXXX, XXX, XXX−XXX